July 9, 2010
Preprint typeset using LaTeX style emulateapj v. 03/07/07

ORIGIN OF THE COMPLEX RADIO STRUCTURE IN BAL QSO 1045+352

Magdalena Kunert-Bajraszewska[1], Agnieszka Janiuk[2], Marcin P. Gawroński[1], Aneta Siemiginowska[3]
[1] Toruń Center for Astronomy, N. Copernicus University, Gagarina 11, 87-100 Toruń,, Poland
[2] N. Copernicus Astronomical Center, Bartycka 18, 00-716 Warsaw, Poland and
[3] Harvard Smithsonian Center for Astrophysics, 60 Garden St, Cambridge, MA 02138

July 9, 2010

ABSTRACT

We present new more sensitive high-resolution radio observations of a compact broad absorption line (BAL) quasar, 1045+352, made with the EVN+MERLIN at 5 GHz. They allowed us to trace the connection between the arcsecond structure and the radio core of the quasar. The radio morphology of 1045+352 is dominated by a knotty jet showing several bends. We discuss possible scenarios that could explain such a complex morphology: galaxy merger, accretion disk instability, precession of the jet and jet-cloud interactions. It is possible that we are witnessing an ongoing jet precession in this source due to internal instabilities within the jet flow, however, a dense environment detected in the submillimeter band and an outflowing material suggested by the X-ray absorption could strongly interact with the jet. It is difficult to establish the orientation between the jet axis and the observer in 1045+352 because of the complex structure. Nevertheless taking into account the most recent inner radio structure we conclude that the radio jet is oriented close to the line of sight which can mean that the opening angle of the accretion disk wind can be large in this source. We also suggest that there is no direct correlation between the jet-observer orientation and the possibility of observing BALs.

Subject headings:

1. INTRODUCTION

Broad absorption lines (BALs) - high ionization resonant lines (C IV 1549$\mathring{A}$) and low ionization lines (Mg II 2800$\mathring{A}$), are seen in a small number (15 %) of both the radio-quiet and radio-loud quasar populations (Dai et al. 2008; Knigge et al. 2008; Gibson et al. 2009), according to the traditional BAL QSO definition of Weymann et al. (1991). They are probably caused by the outflow of gas with high velocities and are part of the accretion process. The presence of BALs is a geometrical effect (Elvis 2000) and/or is connected with the quasar evolution (Becker et al. 2000; Gregg et al. 2000, 2006).

Theoretical models (Elvis 2000; Murray et al. 1995) suggest that BALs are seen at high inclination angles, which means that the outflows from accretion disks are present near the equatorial plane. However, some recent numerical work indicates that it is also plausible to launch bipolar outflows from the inner regions of a thin disk (e.g. Ghosh & Punsly 2007; Proga & Kallman 2004). There is growing observational evidence indicating the existence of polar BAL outflows (e.g. Zhou et al. 2006; Ghosh & Punsly 2008). This means that there is no simple orientation model which can explain all the features observed in BAL quasars.

It has been suggested by Becker et al. (2000) that, because of their small sizes, most of the radio-loud BAL quasars belong to the class of compact radio sources, namely compact steep spectrum (CSS) objects and gigahertz peaked spectrum (GPS) objects. GPS and CSS sources are considered to be young radio sources with linear sizes less than 20 kpc, entirely contained within the extent of the host galaxy. The high resolution observation in the VLBI technique is the best way to learn about their morphologies and orientation. However, very small fraction of compact BAL quasars have been observed with VLBI so far (Jiang & Wang 2003; Kunert-Bajraszewska & Marecki 2007; Liu et al. 2008; Montenegro-Montes et al. 2009, 2008). About half of them still have unresolved radio structures even in the high resolution observations, the others have core-jet structures indicating some re-orientation or very complex morphology, suggesting a strong interaction with the surrounding medium. All of them are potentially smaller than their host galaxies. The analysis of the spectral shape, variability and polarization properties of some of them shows that they are indeed similar to CSS and GPS objects, and are not oriented along a particular line of sight (Montenegro-Montes et al. 2009).

1045+352 is a compact radio-loud CSS source. The spectral observations (Willott et al. 2002) have shown 1045+352 to be a quasar with a redshift of $z = 1.604$. It has also been classified as a HiBALQSO based upon the observed very broad C IV absorption, and it is a very luminous submillimeter object with detections at both 850 μm and 450 μm (Willott et al. 2002). The radio luminosity of 1045+352 at 1.4 GHz is high ($\log L_{1.4\mathrm{GHz}}$=28.25 W Hz^{-1}), making this source one of the most radio-luminous BAL quasars, with a value similar to that of the first known radio-loud BAL QSO with an FR II structure (Gregg et al. 2000). The *Chandra* X-ray observation of 1045+352 (Kunert-Bajraszewska et al. 2009) shows that the X-ray emission of 1045+352 is very weak in comparison to the other radio-loud BAL quasars which, together with the high value of the optical−X-ray index $\alpha_{ox} = 1.88$, suggests the presence of an X-ray absorber close/in the BLR region. The result of the spectral energy distribution (SED) modeling of 1045+352 indicate that the X-ray emission we observe from 1045+352 may mostly be due to X-ray emission from the relativistic jet, while the X-ray emission from the corona is absorbed in a large part. The first multifrequency ra-

TABLE 1
Basic parameters of 1045+352

Parameter	Value
Source name (B1950)	1045+352
RA (J2000) extracted from FIRST	$10^{\rm h}\ 48^{\rm m}\ 34\overset{\rm s}{.}247$
Dec (J2000) extracted from FIRST	$+34^{\rm o}\ 57'.0\ 24''.99$
Redshift z	1.604
Total flux density $S_{1.4\,\rm GHz}$ (mJy)	1051
$\log L_{1.4\rm GHz}$ (W Hz^{-1})	28.25
Total flux density $S_{4.85\,\rm GHz}$ (mJy)	439
Spectral index $\alpha_{1.4\rm GHz}^{4.85\rm GHz}$	0.70
Largest Angular Size measured in the 5 GHz MERLIN image	$0''.5$
Largest Linear Size (h^{-1} kpc)	4.3
Radio-loudness parameter R^*	4.9(4.1)
Intrinsic extinction A_V	1.5
K-corrected absolute magnitude M_V	-22.83(-24.33)

Notes.Quantities in parentheses are corrected for intrinsic extinction. Spectral index defined as ($S \propto \nu^{-\alpha_r}$)

dio observations of the quasar 1045+352 were made by Kunert-Bajraszewska & Marecki (2007). The complex compact structure has been resolved into many subcomponents and indicates that the jet is moving in a non-uniform way in the central regions of the host galaxy. Here we present new, more sensitive, high resolution EVN+MERLIN 5 GHz observations of this source and analyze them.

2. RADIO OBSERVATIONS

1045+352 belongs to the primary sample of 60 candidates for CSS sources selected from the VLA FIRST catalogue (White et al. 1997). Initial observations of all the candidates were made with MERLIN at 5 GHz (Marecki et al. 2003) and 1.7, 5 and 8.4 GHz VLBA follow-up of 1045+352 was carried out on 13 November 2004 in a snapshot mode with phase-referencing (Kunert-Bajraszewska & Marecki 2007). The observations showed that this source has a complex radio morphology with a probable radio jet axis reorientation. To look for the traces of the above-mentioned scenario we planned more sensitive high-resolution EVN+MERLIN 5 GHz observation that was carried out on 2 June 2007 in a full-track mode. The target source itself was observed for 7 hrs. The whole data reduction process was carried out using standard AIPS procedures. IMAGR was used to produce the final images separately for EVN and MERLIN, and finally the combined EVN+MERLIN image was created (Fig. 1). The flux densities of the main components of the target source were then measured, by fitting Gaussian models, using task JMFIT (Table 2). For more extended features the flux densities were evaluated by means of IMSTAT (*, Table 2). The basic parameters of 1045+452 have been gathered in Table 1.

Throughout the paper, we assume the cosmology with H_0=71 km s^{-1} Mpc^{-1}, Ω_M=0.27, Ω_Λ=0.73.

3. RESULTS

Our previous MERLIN image of 1045+352 (Kunert-Bajraszewska & Marecki 2007) shows this source to be extended in both NE/SW and NW/SE directions suggesting a reorientation of the jet axis.

The new EVN+MERLIN 5 GHz radio observations of 1045+352 BAL quasar revealed more details of its complex morphology (Fig. 1). We identify the structure C with the radio core and the structures A - A_3 with the subsequent jet activity. The new 5 GHz EVN observation shows a jet (indicated as a A, Fig. 1a) emerging from the core (C) in the E/SE direction, and then another jet (A_1) emerging in the NE direction. The feature indicated as B is probably a counter-jet, and its trace was also visible in the previous lower resolution 1.7 GHz VLBA image (Kunert-Bajraszewska & Marecki 2007). No corresponding B_1-B_3 structures are found, possibly due to their weakness. There is an appreciable ($\sim 60^{\rm o}$) misalignment between the axis of the inner structure (jet A) with respect to the outer structure (jet A_1). The new combined image shows diffuse radio emission in the center of 1045+352 quasar suggesting very dense medium of the host galaxy of the source and indicating strong interactions (Fig. 1c).

TABLE 2
Flux densities of 1045+352 principal components from the 5 GHz MERLIN and EVN images

Components	MERLIN	EVN	EVN + MERLIN	$\theta_{maj} \times \theta_{min}$
	mJy	mJy	mJy	arcs
A+C	–	104.1 ± 0.4	–	0.01×0.004
A_1	–	51(*)	–	–
A_2	–	–	20(*)	–
A_3	6.0 ± 0.2	–	–	0.06×0.01
B	–	3.8 ± 0.2	–	0.006×0.001

Note. The asterix shows the sum of the visible components.

The projected linear size of the whole structure measured in our old snapshot 5 GHz image (Kunert-Bajraszewska & Marecki 2007) as a size of the contour plot is 4.3 kpc (Table 1). The projected distance between the radio core C and the feature A_3 in the new 5 GHz MERLIN image (Fig. 1b) measured as a separation between the component peaks is 1.7 kpc. The projected size of the innermost part (A+C) is 190 pc. The size of the radio core amounts to 68 pc when measured in the 8.4 GHz VLBA image (Kunert-Bajraszewska & Marecki 2007) where the innermost components were resolved. The measured component fluxes from the 5 GHz EVN and MERLIN images are collected in Table 2.

Based on the higher resolution VLBA image (Kunert-Bajraszewska & Marecki 2007) and using the radio-to-optical luminosity ratio (Wills & Brotherton 1995) we have estimated the angle between the jet axis and the line of sight to be $\theta \sim 30°$. However, this should be treated as a rough approximation since the radio-to-optical luminosity ratio (Wills & Brotherton 1995) was defined for large scale objects and itself suffers from very large uncertainty. In addition, the relation we used is based on the radio luminosity of the core, so we estimate that the derived value of the angle corresponds to the innermost part of the jet - component A.

Component A_3 (Fig. 1b) seems to be the oldest structure of 1045+352. A new emission - radio jet A is emerging from the core C and an earlier phase of the jet activity is represented by components A_1 and B. Because of their symmetry with respect to the radio core, we treated them as jet and counter-jet, respectively. The *jet/counter-jet*

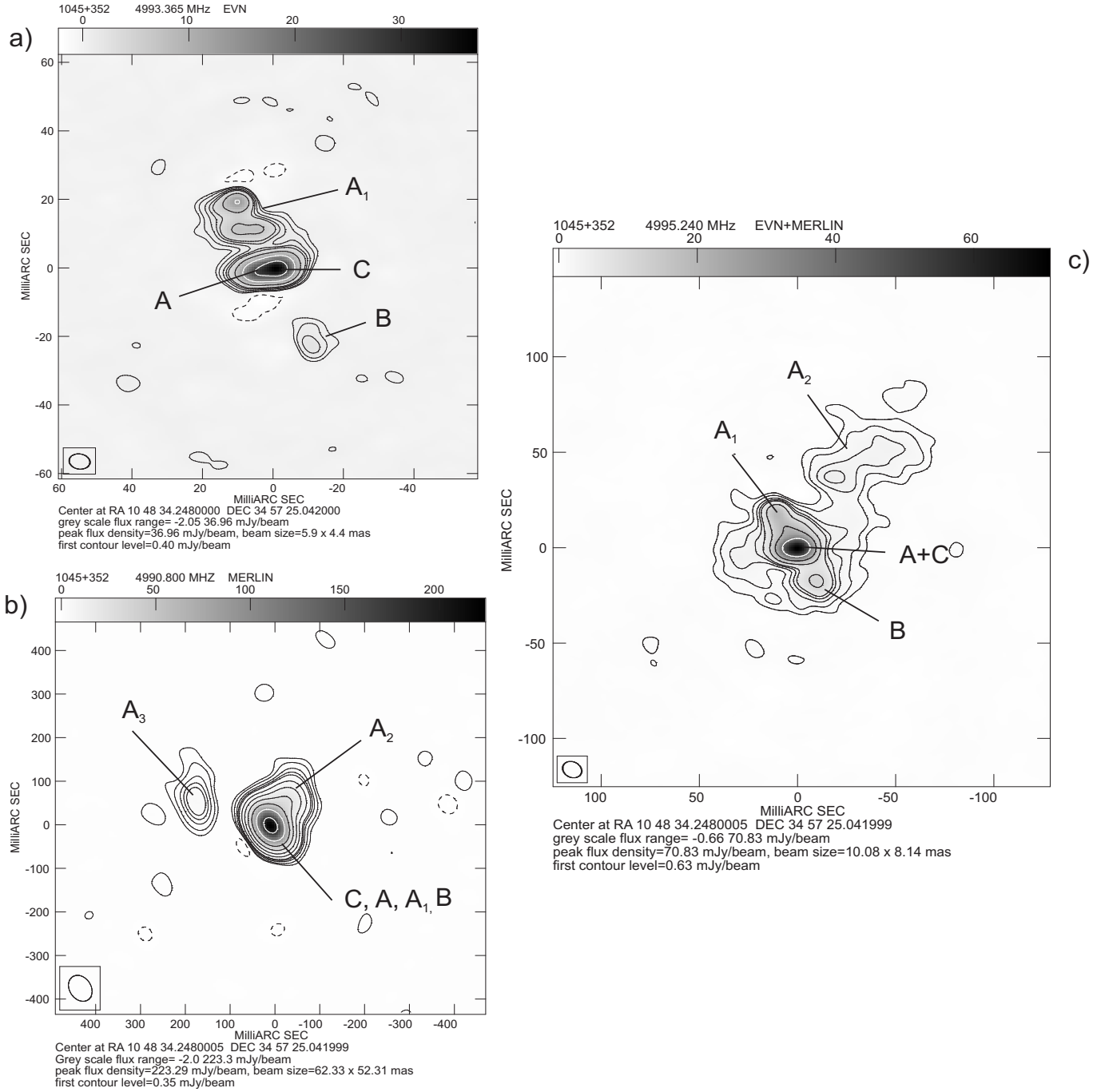

FIG. 1.— Radio images of 1045+352: a) 5 GHz EVN image, b) 5 GHz MERLIN image, c) combined EVN+MERLIN 5 GHz image. Contours increase by a factor 2 and the first contour level corresponds to $\approx 3\sigma$.

brightness ratio is given by:

$$R = \left(\frac{1+\beta cos\Theta}{1-\beta cos\Theta}\right)^{2+\alpha_{jet}} \quad (1)$$

where β is the jet/counter-jet speed, θ is an angle between the jet axis and the line of sight and α_{jet} is the jet average spectral index. The value of the sideness parameter is R $\sim$ 13.5. Then assuming a typical value of the spectral index $\alpha_{jet} = 0.75$ and the jet speed $\beta = 0.9\,c$ we obtained the value of the angle between the jet axis and the line of sight to be $\theta \sim 61°$. However, θ varies in the range $51° - 64°$ for β and α_{jet} values in the range $0.7\,\mathrm{c} - 0.98\,\mathrm{c}$ and $0.7 - 1.1$ respectively. This may indicate a large change between the orientation of 1045+352 radio structures on the different scales and fits well into the picture of complicated radio morphology.

An assumption of $\theta = 30° - 61°$ yields the deprojected linear size of the source of $\sim 5 - 9$ kpc, also indicating a young radio source.

4. DISCUSSION

The complex morphology and a change of the jet direction observed in 1045+352 may result from (1) a merger, (2) a jet precession, or (3) jet-cloud interactions. Below, we discuss possible origins of the multiple radio structures and their misalignment.

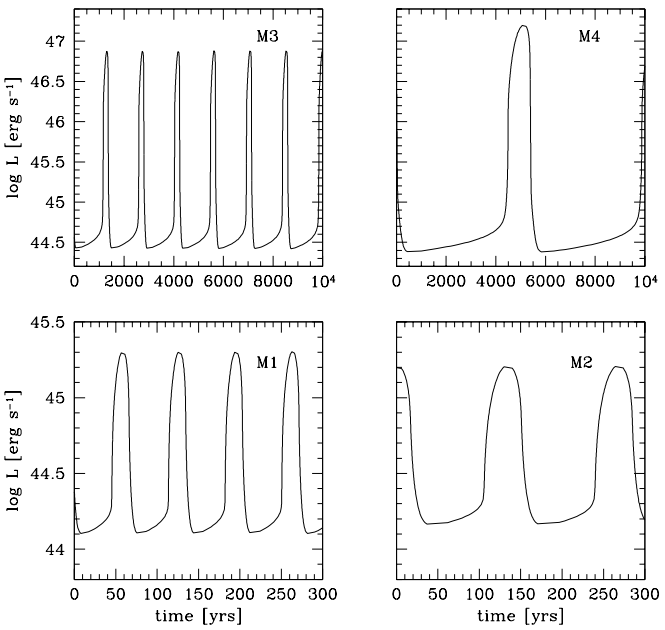

FIG. 2.— The time evolution of the core luminosity for 2 values of mass and the mean accretion rate and 2 values of the viscosity parameter: $\dot{m} = 0.36, 0.68$, $M = 2 \times 10^7, 5.6 \times 10^7 M_\odot$, and $\alpha = 0.03, 0.1$. The parameters are given in the Table 3.

4.1. *Quasar reactivation*

4.1.1. *Galaxy merger*

Observations indicate, that about 50% of young AGN contain double nuclei in their host galaxies or exhibit morphological distortions that are supposed to be due to the past merging events (O'Dea 1998; Liu 2004). Although there are no obvious signs of merger event in the optical image of 1045+352 (from the Sloan Digital Sky Survey, SDSS), the radio distortions indicate this possibility. Therefore we discuss below the possible scenario of a merger event in QSO 1045+352. As shown by Liu (2004), the spin axis of the black hole formed after the merger changes its orientation from the vertical with respect to the outer accretion disk to the aligned with the rotation axis of the binary on timescale 10^5 yr.

The angle by which the jet might have precessed in 1045+352 is difficult to be determined observationally, due to orientation effects. The inclination angle of the A+C structure (jet axis) to the line of sight is about 30°. In the case of the older components A_1 and B it seems to be rather $\theta \sim 61°$. The images of the radio structures are projected onto the plane of the sky. Therefore even for a very small precession angle, e.g. 10°, the misaligned structure will appear shifted by a large angle on the 2-D map, e.g. 90°, due to the projection effect.

In the case of 1045+352, a timescale for the most distant structure A_3 (1.7 kpc, in projection) will be equal to $t = 5.5 \times 10^4$ yrs if we assume the jet velocity of $0.1c$, and $t = 1.8 \times 10^4$ yrs for $0.3c$. Therefore in this source, we may be witnessing an ongoing process of the disk realignment after a merger event, which took place after structure A_3 was ignited.

4.1.2. *Accretion disk instability*

TABLE 3
MODELS OF THE ACCRETION DISK EVOLUTION

Model	α	$\dot{m}$ [$\dot{M}_{\rm Edd}$]	$M[M_\odot]$	$T_{\rm q}$ [yrs]	$T_{\rm out}$ [yrs]
M1	0.1	0.36	2×10^7	45	25
M2	0.03	0.36	2×10^7	85	45
M3	0.1	0.68	5.6×10^7	$1.75{\times}10^3$	235
M4	0.03	0.68	5.6×10^7	$4.35{\times}10^3$	880
A1	0.01	1.0	4×10^8	$8.5{\times}10^4$	$2.05{\times}10^4$
A2	0.01	0.7	4×10^8	$1.5{\times}10^4$	$8.1{\times}10^3$
B1	0.1	1.0	4×10^8	$3.8{\times}10^4$	$4.8{\times}10^3$
B2	0.1	0.7	4×10^8	$2.5{\times}10^4$	$1.8{\times}10^3$

Totes. α - viscosity parameter, $T_{\rm q}$ - quiescent time, $T_{\rm out}$ - outburst time.

In this section, we apply the accretion disk instability model to explain the "reactivation" of the 1045+352 core. Below, we describe in brief the basic properties of this model, which was described in more detail elsewhere (Janiuk et al. 2002; Czerny et al. 2009).

Instabilities of the accretion disks have been shown to operate on long (Siemiginowska et al. 1996; Janiuk et al. 2004; Janiuk & Czerny 2007) and short timescales (Janiuk et al. 2002; Czerny et al. 2009) , depending on their nature (the dwarf-nova type of instability, caused by the partial ionization of hydrogen; or the radiation pressure instability, studied in microquasars). Scaling the outbursts of the Galactic microquasar GRS 1915+105, lasting about 100−2000 seconds for a black hole mass of $10M_\odot$, to the quasar hosting a supermassive black hole, gives outbursts on timescales of $10^2 - 10^5$ years.

The unstable disk surrounding a black hole is subject to thermal and viscous instability if the radiation pressure dominates over the gas pressure. If the accretion rate outside the unstable region (i.e. the mean accretion rate) is such that the disk is in the unstable mode, the source enters a cycle of bright, hot states, separated by cold, quiescent states. In the hot state, the luminous quasar could power a radio jet, while during the cold state the radio activity ceases.

The quantitative results, i.e. the outburst amplitudes and durations, are sensitive to the model parameters: black hole mass and viscosity coefficient. In addition, the description of the heating is essential. If the heating is proportional to the total pressure, the outburst amplitudes are very large. The heating proportional to the square root of the gas times the total pressure reduces the amplitude of the disk outbursts.

We compute the time dependent accretion disk model for several combinations of the main parameters: four values of the mean accretion rate, $\dot{m} = 0.36, 0.68, 0.7$ and 1.0 in units of the Eddington accretion rate; three values of the viscosity parameter: $\alpha = 0.01, 0.03$ and 0.1; and three values of the black hole mass, $M = 2{\times}10^7, 5.6{\times}10^7$ and $4 \times 10^8 M_\odot$ (see Table 3; models are labeled with A, B, and M). The accretion rate is in the units of the Eddington accretion rate, $\dot{M}_{\rm Edd}$, which corresponds to the Eddington luminosity. In Table 3 we give the resulting time for the quiescent and outburst periods. In Figure 2 we show the exemplary light curves from the time dependent accretion disk model. In general, the outburst separation is consistent with the one required by Reynolds & Begelman (1997), who proposed a phenomenological model to fit the observed number of radio sources and their sizes.

In our model, for a given black hole mass, the larger the mean accretion rate, the longer the duration of a cycle episode, both in hot and cold states. In addition the α parameter affects the results and for smaller viscosity, the cycle duration is longer. This relation was calibrated by Czerny et al. (2009) using a grid of models for various black hole masses and Eddington ratios. The proper value of a bolometric correction in this relation can give us an estimation of an upper limit for the age of a radio source (i.e. the duration of the hot state). The predicted timescales and durations are in agreement with observations of compact radio sources (Wu 2009).

The outbursts are associated with the ejections of radio jets. The jets are then turned-off between the outbursts and each radio structure will represent a new outburst. In case of an apparently young, compact source we can suspect that in fact it is an old, reactivated object, in which the vast radio structures have already faded away and are not visible. This mechanism would explain the apparent statistical excess of the compact sources with respect to the galaxies with extended radio structures (O'Dea & Baum (1997)). On the other hand, the timescales for fading of a radio source may be much longer than the separation timescales between the outbursts and we should observe the fossil radio structures in addition to the compact one (Baum et al. 1990). These kind of morphologies have already been observed in large scale objects showing evidence of two or more active periods (e.g Schoenmakers et al. 2000; Jamrozy et al. 2007).

Here, we present the results of the modeling of the intermittent activity for the source 1045+352. The best fitting parameters for the quasar 1045+352 from Kunert-Bajraszewska et al. (2009) were $M_{BH} = 2 \times 10^7 M_\odot$, $\dot{m} = 0.36$ and $\alpha = 0.1$ (model M1). Such a large accretion rate is high enough for the radiation pressure instability to operate ($\dot{M}_{\rm crit} \approx 0.2 M_{\rm Edd}$). We take these parameters as an input to our time-evolution computations, and for comparison we calculate model M2, with a different viscosity. The accretion rate in solar masses per year is therefore $\dot{M} = \dot{m} \times 3.52\, M_8 = 0.253\, M_8$, where M_8 is the black hole mass in the units of 10^8 Solar masses. Because the black hole mass determination for this source is not very certain, and seems to be rather a lower limit, we calculated also several models for somewhat larger masses (models M3, M4, for which we used the mass estimation from the monochromatic luminosity; models A and B, where the assumed mass value enables the radio source to escape from the host galaxy). The model is quite sensitive for the adopted central mass value and the results presented here are only examples. Full parameter space for the mass and accretion rates for large sample of quasars was presented in Czerny et al. (2009).

In the bottom left panel of Fig. 2 we plot the light curve for the given best fit parameters, taken from the spectral modeling (Kunert-Bajraszewska et al. 2009). The parameters are given in the Table 3, model M1. The resulting duration of an active phase in this case would be about 25 years, while for the quiescent phase it is about 45 years (see Czerny et al. 2009) for the dependence between the activity timescale and bolometric luminosity of the source).

In this scenario, the subsequent radio structures would be fed by the jet produced during the active phase of the central engine. In the quiescent phase, the jet stops feeding the radio lobe, and further expansion of the remnant radio structure proceeds due to the accumulated jet energy. If the proper motion of the outer jet components in 1045+352 is in the order of $0.1 - 0.2\, c$, and the restart of the activity was after $T_{\rm q} \sim 50$ yrs, then the physical separation of the radio structures would be of about 10 pc. If the velocities of the jet were rather of $0.7 - 0.9\, c$, such as those characteristic of the inner structures A_1 - B, then this separation would increase to 35−45 pc.

During the active phase, the radio lobes are fed by the expanding jet and the source grows. For the outburst duration calculated in model M1, the size of the central radio core would be only about 1.5 pc for a jet velocity of $0.1\, c$, 4.6 pc for velocity of $0.3\, c$ and 15 pc for a relativistic jet speed of $0.9\, c$. The resulting size of the radio source is therefore too small in comparison with the structure size estimated from our images (the size of the radio core is ∼70 pc). The much larger actual size requires longer activity timescales, which are possible in the models with larger black hole mass and accretion rate and/or smaller viscosity. We therefore checked a number of additional models, with larger black hole mass and accretion rate. In particular, the subsequent models M2, M3 and M4 adopt these parameters within the range of the plausible values for our previous spectral modeling. These values were not the best fit, however, they also gave a reasonable shape of the high energy spectrum of this quasar and therefore cannot be excluded. As Table 3 shows, model M4, with black hole mass of $5.6 \times 10^7 M_\odot$, accretion rate of $\dot{m} = 0.68$ and viscosity $\alpha = 0.03$ results in an outburst timescale of almost 900 years, which gives a size of the radio core of 30−80 pc, depending on the jet velocity (non-relativistic). This is in good agreement with the estimated size of the central radio core. On the other hand, if the jet velocity is relativistic, the models with smaller black hole mass would be favored, consistent with the spectral fitting results.

The above model of the cyclic activity of the central core is based on the 1-D, vertically averaged calculations and does not describe any effects in the polar direction. Therefore the jet axis assumed to be perpendicular to the disk plane is constant in time, and the subsequent radio structures should be co-aligned. Taking into account, that the lobe separation is much smaller than the distance to the source, the viewing angle of $\theta \sim 30^\circ$ between the line of sight and the younger radio lobe would be practically the same as the angle to the older lobe. In the case of 1045+352 the parts of the jet we observed in the 5 GHz structure are not co-aligned. Structures A_1 - A_2 are shifted with respect to the core, while the structure A_3 is misaligned by a large angle.

4.2. *Precession of the jet*

The observed misalignment between the young and old radio structures could be the result of the changed direction of the jet axis between the activity episodes. The precession of the jet could be caused by various mechanisms, such as tidal forces, disk warping, irradiation, and the Bardeen-Petterson effect (Caproni et al. 2006). In this section, we consider the precession of the innermost accretion disk due to internal instabilities within the accretion flow. As studied by Janiuk et al. (2008, 2009), acoustic instabilities of the Papaloizou-Pringle type can

arise in the highly supersonic inner parts of the accretion flow. The azimuthal modes of such instabilities will lead to the initially differential tilt of the rotating torus and its subsequent precession. The 3-D hydrodynamic simulations were performed to determine the rate of such precession, which is dependent on the adopted equation of state (i.e. the gas adiabatic index), and scales with the black hole mass.

In Figure 3 we show the precession angle as a function of time, for $M_{BH} = 2 \times 10^7 M_\odot$. The simulations were performed for a few equations of state, and we show here only the result for the adiabatic index $\gamma = 5/3$, which corresponds to the gas pressure dominated case. The twist angle, shown in the Figure as a function of time, is defined as follows:

$$\gamma(r,t) = \arccos\Big(\frac{L_z}{\sqrt{L_x^2 + L_y^2}}\Big). \qquad (2)$$

where $L_{\rm x}$, $L_{\rm y}$ and $L_{\rm z}$ are the Cartesian components of the angular momentum vector. The twist is therefore defined as a cumulative angle by which the angular momentum vector revolves in the $x-y$ plane by the time t.

Initially, when the torus is axisymmetric and no tilt occurs, the only component of the angular momentum vector is $L_{\rm z}$ and its sign depends on the direction of the flow rotation. When the torus tilts, the non-zero $L_{\rm x}$ and $L_{\rm y}$ components appear and the rotation axis tilts toward the $x-y$ plane. Initially, the torus precession is differential and the twist angle rises fast mostly in the innermost parts of the flow. In the Figure 3, we show the twist averaged over radius between the inner edge and 50 Schwarzschild radii. The twist angle decreasing from $\sim 60^\circ$ to $\sim -80^\circ$ in the innermost torus reflects the clockwise precession. The moment, when the precession starts during the hydrodynamic simulation, as well as the period of precession, depend on the model (i.e. on the equation of state). For the model shown here, we estimated that the precession period is 2.4×10^4 in the units of dynamical time at the inner radius. For the black hole mass of $2 \times 10^7 M_\odot$ it is about 2.5 years

The simulations we described above assume a radiatively inefficient flow, and therefore they are adequate for the quiescent state of the central core of the quasar. In other words, the accretion rate in the precessing disk is negligibly small, and as such is not taken into account in the 3-D modeling. Accordingly, we postulate here that the precession of the disk occurs between the activity episodes, and each subsequent episode restarts the jet production along a misaligned axis. The direction of the axis is basically random, because the period of precession is much smaller (about 20 times) than the duration of the quiescent phase. In consequence, the younger radio structure is easily formed at a different angle to the line of sight than the older one and the probability of that is very high taking into account the very small precession period.

We note that this approach is a simplification and in order to really model the precession effect we would need to compute the 3-dimensional model with somewhat higher accretion rate and radiative efficiency. This is beyond the scope of our present computations. However, based on the results of Das (2004), we suppose that at least for not extremely large accretion rates and viscosities, the effect of precession would be enhanced, because of the outward shifting of the sonic point.

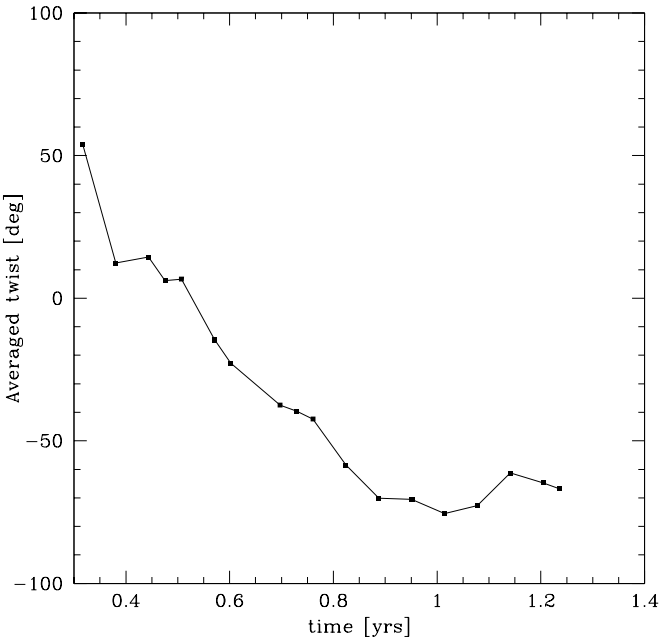

FIG. 3.— The twist angle averaged over radius, from 1.5 to 50 $R_{\rm Schw}$, as a function of time. The black hole mass is $2 \times 10^7 M_\odot$.

4.3. *Interaction with the interstellar medium*

The repetitive outbursts of the central core due to the accretion disk instability may potentially have a strong impact on the ISM. Due to the cyclic irradiation from the central UV source, the shocks in the ISM may arise on short timescales and keep the gas warm. The hot spots can travel to a certain distance within the host galaxy, before the outburst is finished. This depends on the outburst duration and in case of a short timescale the radio source does not expand beyond the host galaxy. According to Czerny et al. (2009) in order for the source to escape the host galaxy the outburst would need to be longer than 10^4 yrs. For 1045+352, however, this would require a large black hole mass in this quasar, $M = 4 \times 10^8 M_\odot$, an accretion rate equal to the Eddington limit, and a very small viscosity (models A and B in Fig. 3). Such values were excluded by our previous spectral modeling (Kunert-Bajraszewska et al. 2009). In particular, for 1045+352, the estimated core size is about 70 pc.

After the jet activity in 1045+352 ceases the radio structure will be driven further due to the pressure expansion, up to a distance of about 1 kpc (for the ISM density of $n = \rho/m_{\rm p} = 0.1$ cm^{-3}, its temperature of 10^7 K and the jet power of $L_{\rm jet} = 10^{44}$ erg s^{-1} (Kunert-Bajraszewska & Marecki 2007)), assuming that the accumulated jet energy is comparable to the energy content in the heated medium, $E = R^3 \rho c_{\rm s}^2 \sim L_{\rm jet} t$ (Stawarz et al. 2008). This distance is comparable to that of the outermost radio structure, A_3 in our map (1.7 kpc). If the jet power was somewhat smaller, the distance of the radio structures driven by the pressure expansion would also be smaller, and could be comparable to the inner component A_2 as well.

When the expansion stops, the radio structure will start recollapsing. The recollapse time is typically much longer than the outburst cycle, and the "tunnel" made by the expanding jet will not close before the next outburst. (For our favorable parameters, the next outburst will start after about 4×10^3 years.) Therefore the jets will always propagate into a rarefied medium. This would imply that the jet is propagating with a large velocity, and thus the velocity of $> 0.1\,c$ would be favored (Stawarz 2004). In this case, any distortions in the jet morphology would propagate rather quickly and the apparent twist seen in the maps (i.e. structure A_3) could be enhanced. It has to be noted however, that there is a large uncertainty in the measurements of a black hole mass. According to the SED modeling the value of the black hole mass in 1045+352 is on the order of $10^7 M_\odot$, according to the Mg II λ2800 FWHM it is on the order of $10^8 M_\odot$. We therefore cannot exclude the possibility that the radio structure of 1045+352 will be able to escape from the host galaxy during this phase of the radio jet activity.

Our analysis of radio components observed in 1045+352 may suggest the following interpretation: the radio jet emerging from the core in a E/SE direction is not able to get through the dense environment and bends to NE direction (component A_1). The radio emission indicated with A_2 (Fig. 1c) and visible in a NE direction is probably another trace of jet-cloud interaction. Its continuation (A_3) is visible on the MERLIN 5 GHz image (Fig. 1b). The weakness of the counter-jet emission is probably caused by the large beaming. However, the structure may be as well interpreted as involving at least three phases of quasar activity: components A_2-A_3 as the oldest one, structure A_1-B as the younger one, and the jet A as the current activity direction.

4.4. *Radio structures of BAL quasars*

Observations based on the VLA FIRST survey have revealed the existence of radio-loud BAL quasars (Becker et al. 2000; Menou et al. 2001), which together with the 5 radio-loud BAL quasars from NVSS discovered by Brotherton et al. (1998) make a large population of objects, about 14%-18% of the total sample of Becker et al. (2000). There are only ten known radio-loud BAL quasars with the extended double-lobed radio emission (Wills et al. 1999; Gregg et al. 2000, 2006; Brotherton et al. 2002; Zhou et al. 2006). Among these are: FR II quasar with a steep spectrum core suggesting restarted activity inside (Gregg et al. 2000), a hybrid object whose morphology indicates some type of jet-medium interactions (Wills et al. 1999), and a very core-dominated radio triple, probably beamed source (Brotherton et al. 2002). However, most of the BAL quasars remain unresolved even with the VLBI observations (Montenegro-Montes et al. 2009; Doi et al. 2009). This implies they are either beamed with the jet pointing close to the line of sight, or they are very compact objects starting their activity. The resolved ones show complex double or triple, in many cases asymmetric, morphology. In general, the radio-loud BALs tend to be compact in the radio, similar to GPS and CSS sources, which are thought to be the young counterparts of powerful large-scale radio sources (Becker et al. 2000). They have wide range of spectral indices which together with the polarization properties suggest that the radio-loud BAL quasars are not oriented along a particular line of sight (Becker et al. 2000; Montenegro-Montes et al. 2009), contrary to the orientation model. The evolution interpretation of the nature of BAL phenomena is also still discussed.

1045+352 is a radio-loud BAL quasar and CSS object with a very complex structure which suggests that the radio jet is oriented close to the line of sight. Morphologies like that observed in 1045+352 are seen among other CSSs (e.g. Fanti et al. 2002; An et al. 2010), although they are not very common. It is very likely that many CSS objects interact with an asymmetric medium in the central regions of their host galaxies, and this can cause the observed asymmetries and distortions (Saikia et al. 2001; Jeyakumar et al. 2005). In the case of 1045+352 an additional fact may matter, namely, thar our *Chandra* X-ray observations suggest a presence of the absorbing material (Kunert-Bajraszewska et al. 2009) close/in the BLR region. It is then possible that the outflowing material detected in absorption may also have interacted with the radio jet disturbing its structure (see also the interpretation of the radio morphology of CSS quasar 3C48 by Gupta et al. (2005)). Such a strong interaction between a relativistic jet and a BAL wind has been reported in Mrk 231 (Reynolds et al. 2009), although the interaction takes place at the small deprojected distance of ~ 4 pc from the radio core.

Recently Shankar at al. (2008) studied the radio properties of BAL quasars based on the SDSS/DR3 and FIRST surveys and found that the number of classical BAL QSOs decreases with increasing radio power. They discussed several plausible physical models which may explain the observations, namely the evolution and orientation model, however none of them can fully explain all the features and correlations observed among radio-loud BAL quasars. As has already been suggested (Elvis 2000) not only equatorial disk wind but also cone outflows can be responsible for BAL features. Thus an internal orientation effect such as the opening angle of the accretion disk wind instead of the external orientation effect such as an angle between the jet axis and our line of sight, could be what determines a possibility of observing any BAL features.

The discussed orientation of 1045+352 is not in agreement with the orientation model, however, the BAL features are clearly visible in this source. After Kunert-Bajraszewska et al. (2009) we suggest that there is no a direct dependence between the radio jet orientation and the probability of BAL visibility.

5. SUMMARY

1045+352 is a CSS object and a HiBAL quasar at a medium redshift. The spectrum classification and linear size of the source indicate that it is a young object in the early phase of its evolution. The new more sensitive high-resolution EVN+MERLIN 5 GHz observations revealed details of the source radio emission and confirmed its complicated radio structure. The radio morphology of 1045+352 is dominated by the strong radio jet resolved into many subcomponents and changing its orientation during propagation in the central regions of the host galaxy. The presence of the dense environment and material outflows have been already confirmed in

this source based on the submillimeter and X-ray observations and as we discussed, they can have a significant impact on the radio jet morphology of 1045+352. We conclude that the most probable interpretation of the observed radio structure of 1045+352 is the ongoing process of the jet precession due to internal instabilities within the flow and/or jet interaction with a dense, inhomogeneous interstellar medium.

It is difficult to establish the orientation between the jet axis and the observer in 1045+352 because of the complex structure. Nevertheless taking into account the innermost radio structure we suggest that the radio jet is oriented close to the line of sight. This means that the opening angle of the accretion disk wind can be large in this source.

We thank Peter Thomasson for his help with MERLIN observations and data reduction. MERLIN is a UK National Facility operated by the University of Manchester on behalf of STFC.

We thank Zsolt Paragi and Bob Campbell for their help with EVN data reduction. The European VLBI Network is a joint facility of European, Chinese, South African and other radio astronomy institutes funded by their national research councils.

This work was supported by the Polish Ministry of Science and Higher Education under grant N N203 303635.

REFERENCES

An, T., Hong, X. Y., Hardcastle, M. J., Worrall, D. M., Venturi, T., Pearson, T. J., Shen, Z.-Q., Zhao, W., Feng, W. X., 2010, MNRAS, 402, 87
Baum, S. A., O'Dea, C. P., Murphy, D. W., & de Bruyn, A. G. 1990, A&A, 232, 19
Becker, R. H., White, R. L., Gregg, M. D., Brotherton, M. S., Laurent-Muehleisen, S. A.; Arav, N., 2000, ApJ, 538, 72
Brotherton, M. S., van Breugel, W., Smith, R. J., et al. 1998, ApJ, 505, L7
Brotherton, M. S., Croom, S. M., De Breuck, C., Becker, R. H., Gregg, M. D., 2002, AJ, 124, 2575
Caproni, A., Livio, M., Abraham, Z., Mosquera Cuesta, H. J. 2006, ApJ, 653, 112
Czerny B., Siemiginowska, A., Janiuk A., Nikiel-Wroczynski B., Stawarz Ł., 2009, ApJ, 698, 840
Dai, X., Shankar, F., Sivakoff, G. R., 2008, ApJ, 672, 108
Das, T., 2004, MNRAS, 349, 375
Doi, A., et al., 2009, PASJ, 61, 1389
Elvis, M. 2000, ApJ, 545, 63
Fanti, C.; Fanti, R.; Dallacasa, D.; McDonald, A.; Schilizzi, R. T.; Spencer, R. E, 2002, A&A, 396, 801
Ghosh, K. K. & Punsly, B., 2007, ApJ, 661, L139
Ghosh, K. K. & Punsly, B., 2008, ApJ,674, L69
Gibson, R. R., Jiang,L., D. P., Brandt, W. N., et al., 2009, ApJ, 692, 758
Gregg, M. D., Becker, R. H., Brotherton, M. S., Laurent-Muehleisen, S. A., Lacy, M., White, R. L., 2000, ApJ, 544, 142
Gregg, M. D., Becker, R. H., de Vries, W., 2006, ApJ, 641, 210
Gupta, N., Srianand, R., Saikia, D. J., 2005, MNRAS, 361, 451
Jamrozy, M., Konar, C., Saikia, D.J., Stawarz, Ł., Mack, K.-H., Siemiginowska, A., 2007, MNRAS, 378, 581
Janiuk A., Czerny B., Siemiginowska A., 2002, ApJ, 576, 908
Janiuk, A., Czerny B., Siemiginowska A., Szczerba R., 2004, ApJ, 602, 595
Janiuk, A., Czerny B., 2007, A&A, 466, 793
Janiuk A., Proga D., Kurosawa R., 2008, ApJ, 681, 58
Janiuk A., Sznajder M., Moscibrodzka M., Proga D., 2009, ApJ, 705, 1503
Jiang, D. R., & Wang, T. G. 2003, A&A, 397, L13
Jeyakumar, S., Wiita, P. J., Saikia, D. J., Hooda, J. S., 2005, A&A, 432, 823
Knigge, C., Scaringi, S., Goad, M. R., Cottis, C. E., 2008, MNRAS, 386, 1426
Kunert-Bajraszewska, M., Siemiginowska, A., Katarzyński, K., Janiuk, A., 2009, ApJ, 705, 1356
Kunert-Bajraszewska, M., & Marecki, A., 2007, A&A, 469, 437
Liu, F. K., 2004, MNRAS, 347, 1357
Liu, Y., Jiang, D. R., Wang, T. G., Xie, F. G. 2008, MNRAS, 391, 246
Marecki, A., Spencer, R. E., & Kunert, M.: 2003, PASA 20, 46
Menou, K., Vanden Berk, D. E. & Ivezic 2001, ApJ, 561, 645
Montenegro-Montes, F. M., Mack, K.-H., Benn, C. R., Carballo, R., Gonzlez-Serrano, J. I., Holt, J., Jimnez-Lujn, F., 2009, AN, 330, 157
Montenegro-Montes, F. M., Mack, K.-H.; Vigotti, M.; Benn, C. R.; Carballo, R.; Gonzlez-Serrano, J. I.; Holt, J.; Jimnez-Lujn, F., 2008, MNRAS, 388, 1853
Murray, N., Chiang, J., Grossman, S. A., Voit, G. M., 1995, ApJ, 451, 498
O'Dea, C. P., & Baum, S. A., 1997, AJ 113, 148
O'Dea, C. P. 1998, PASP, 110, 493
Proga, D. & Kallman, T. R., 2004, ApJ, 616, 688
Reynolds, C., Punsly, B., Kharb, P., O'Dea, C. P., Wrobel, J., 2009, ApJ, 706, 851
Reynolds, C. S., & Begelman, M. C., 1997, ApJ, 487, L135
Saikia, D. J., Jeyakumar, S., Salter, C. J., Thomasson, P., Spencer, R. E., Mantovani, F., 2001, MNRAS, 321, 37
Shankar, F., Dai, X., Sivakoff, G. R., 2008, ApJ, 687, 859
Schoenmakers, Arno P.; de Bruyn, A. G.; Rttgering, H. J. A.; van der Laan, H.; Kaiser, C. R., 2000, MNRAS, 315, 371
Siemiginowska A., Czerny B., Kostyunin V., 1996, ApJ, 458, 491
Stawarz L., 2004, ApJ, 613, 119
Stawarz, L., Ostorero, L., Begelman, M. C., Moderski, R., Kataoka, J., Wagner, S., 2008, ApJ, 680, 911
Weymann, R. J., Morris, S. L., Foltz, C. B., & Hewett, P. C. 1991, ApJ, 373, 23
White, R. L., Becker, R. H., Helfand, D. J., & Gregg, M. D. 1997, ApJ, 475, 479
Willott, C. J., Rawlings, S., Archibald, E. N., Dunlop, J. S., 2002, MNRAS, 331, 435
Wills, B. J., & Brotherton, M. S., 1995, ApJ, 448, L81
Wills, B. J.,Brandt, W. N., Laor, A., 1999, ApJ, 520, L91
Wu Q., 2009, ApJ, 701, L95
Zhou, H., Wang, T., Wang, H., Wang, J., Yuan, W., Lu, Y., 2006, ApJ, 639, 716